EurJIC
European Journal of Inorganic Chemistry

Full Papers
doi.org/10.1002/ejic.202100359

Chemistry Europe
European Chemical Societies Publishing

Iron(III) Complexation with Galactodendritic Porphyrin Species and Hydrocarbons' Oxidative Transformations

Kelly A. D. F. Castro,[a, b] Kátia C. M. Westrup,[a] Sandrina Silva,[b] Patrícia M. R. Pereira,[b] Mário M. Q. Simões,[b] Maria da Graça P. M. S. Neves,[b] José A. S. Cavaleiro,[b] João P. C. Tomé,*[c] and Shirley Nakagaki*[a]

The iron metalation of the known free-base porphyrins **H_2P2** and **H_2P3**, obtained by structural modification of the well-known $TPPF_{20}$ (**H_2P1**) with galactose dendritic units, gave the corresponding iron(III) porphyrin complex **FeP2** and the solid hybrid material **FeP3S**. Their synthesis, characterization and catalytic efficacy toward the oxidation of the organic substrates (*Z*)-cyclooctene, cyclohexane and heptane, are reported. In this work, the possibility to modulate selectivity and chemical efficiency of the catalytic system by using simple and more sophisticated metalloporphyrins is demonstrated. Furthermore, the presence of the galactose dendrimer units at the *meso*-porphyrin ring positions can tune the oxidation at the terminal positions in linear alkanes. In addition, the **FeP3S** material was easily recovered and reused at least 3 times for the cyclooctene oxidation. The catalytic performance of material **FeP3S**, associated with their possibility of reuse, makes this material a promising catalyst.

1. Introduction

Porphyrin derivatives are usually known as "pigments of life" due to their role in important vital functions such as photosynthesis, respiration and detoxification of xenobiotics.[1] However, with the development of new synthetic derivatives, namely of synthetic origin, the interest of the scientific community in such compounds was extended to potential significant applications in various fields, particularly in medicine[2] and catalysis.[3]

Green chemistry and catalysis in synthetic chemistry approaches have challenges, envisaging transformations favoring the selective preparation of products of commercial interest, minimizing the formation of byproducts and wastes.[4] The development of selective and efficient catalysts for the oxidation of alkanes and alkenes in a green chemistry perspective[4a] is of great importance, since such reactions have wide applications in industrial processes.[3j,5] Moreover, the search for catalysts able to promote the selective oxidation of organic compounds under mild conditions, minimizing the waste formation and the possible damage to the environment, is one of the most significant challenges chemistry today.[6]

The epoxides obtained by selective oxidation of olefins are highly useful intermediates for the manufacture of important commercial products such as polyurethanes and polyamides, epoxy resins, polyesters, among others.[7] Regarding the oxidation of alkanes, the mixture of cyclohexanone and cyclohexanol (KA-oil) from the selective oxidation of cyclohexane is very attractive due to its importance as intermediate in manufacturing Nylon-6 and Nylon-6,6.[8]

Understanding the role of different metal complexes in biological processes, namely to perform enzymatic reactions, is a scientific challenge and frequently an inspiration to develop catalysts for different reactions with potential industrial applications.[9] Based on effective catalytic biologic systems, synthetic but bioinspired catalytic systems have been proposed and studied over the last decades.[3f,k,m,10] For example, inspired by the efficiency and selectivity of the reactions catalyzed by the cytochrome P-450 enzymatic system, different synthetic metalloporphyrins have been prepared and investigated as oxidative catalysts for oxidation reactions over the years.[3k,l,o,p,11] Despite several studies, only a few promising porphyrin complexes have pointed out a putative future industrial use of these molecules.[12] Investigations have shown that electronegative and/or bulky substituents at the *meso* positions of the porphyrins' ring (second generation porphyrins)[3m,13] are key features leading to more robust catalysts, resistant to degradation of the porphyrin macrocycle during catalysis and, consequently, to a better catalytic performance. It has also been observed that the selectivity to a desired product may often require a certain degree of sophistication in the design of specific catalysts.[3f,g,14]

Taking all that into account, we report here the iron metalation, characterization and preliminary catalytic studies involving the novel iron(III) porphyrin **FeP2** and the insoluble

[a] *Dr. K. A. D. F. Castro, Dr. K. C. M. Westrup, Prof. Dr. S. Nakagaki*
Laboratório de Química Bioinorgânica e Catálise,
Universidade Federal do Paraná (UFPR),
CP 19061, CEP 81531-980, Curitiba, Paraná, Brazil
E-mail: shirleyn@ufpr.br
[b] *Dr. K. A. D. F. Castro, Dr. S. Silva, Dr. P. M. R. Pereira,*
Prof. Dr. M. M. Q. Simões, Prof. Dr. M. d. G. P. M. S. Neves,
Prof. Dr. J. A. S. Cavaleiro
LAQV-REQUIMTE, Department of Chemistry,
University of Aveiro,
3810-193 Aveiro, Portugal
[c] *Prof. Dr. J. P. C. Tomé*
Centro de Química Estrutural, Instituto Superior Técnico,
Departamento de Química, Universidade de Lisboa
Av. Rovisco Pais, 1049-001 Lisboa, Portugal
E-mail: jtome@tecnico.ulisboa.pt

Supporting information for this article is available on the WWW under https://doi.org/10.1002/ejic.202100359

Part of the "Inorganic Chemistry in Latin America" Special Collection.

hybrid material **FeP3S**, obtained from the corresponding free-base galactodendritic porphyrins **H_2P2** and **H_2P3** (Scheme 1).[15] The organic substrates (*Z*)-cyclooctene, cyclohexane and heptane were selected to evaluate their performance as catalysts in epoxidation and hydroxylation processes and the results were compared with those obtained when using the iron(III) complex of 5,10,15,20-tetrakis(pentafluoroporphyrin), **FeP1**. The galactose dendrimer units at the *meso*-porphyrin positions were found to be important to promote the oxidation results observed *e.g.* the oxidation at terminal positions in linear alkanes.

2. Results and Discussion

Synthesis and characterization of the iron(III) porphyrins FeP2 and FeP3S

The reaction of porphyrins **H_2P2** and **H_2P3** bearing protected and unprotected galactose units with iron(II) chloride afforded the complex **FeP2** and the insoluble material **FeP3S** (Scheme 2).

These free-base porphyrins were obtained from 5,10,15,20-tetrakis(pentafluorophenyl)porphyrin (**H_2P1**) according to a synthetic methodology previously reported by our group (Scheme 1).[3g,15] The nucleophilic substitution of the four *p*-fluorine atoms of the C_6F_5 groups with the adequate thiol galactodendritic unit provided porphyrin **H_2P2** first and then porphyrin **H_2P3**, after the removal of the galactose protecting groups.[3g,15]

The **FeP1** complex obtained from the starting porphyrin **H_2P1** was also considered for comparison. The UV-Vis spectrum of **FeP1** showed the expected spectral features – a Soret band at 414 nm, which is slightly red-shifted when compared to the Soret band of the precursor **H_2P1** (409 nm) and a lower number of Q-bands (506 nm, 566 nm and 624 nm). The band observed at 348 nm can be attributed to the coordination of the chloride ion to iron(III) (see Figure S1 and Figure S2, Supporting information).[16] The coordination of the free-base **H_2P2** (Scheme 2) with the iron(III) ion was accompanied by spectral changes in its UV-Vis spectrum (Figure S3) similar to those observed between **FeP1** and **H_2P1**.[3c,f,17] The characteristic Soret band appears slightly red shifted for **FeP2** when compared with the free-base porphyrin (414 nm *versus* 410 nm) and this shift was also accompanied by a decrease in the number of the Q-bands (appearing at 505, 584 and 648 nm), resulting from the modification in the microsymmetry of the porphyrin macrocycle from D_{2h} to D_{4h}[17b] (Figure S3, Supporting information).

The metalation of **H_2P3** with an excess of iron(II) chloride, using a similar methodology to that described for **H_2P1** and **H_2P2** brought forth, at the end of the reaction, the precipitation of a dark purple solid designed as **FeP3S**. This solid showed a different solubility profile in comparison to the free-base porphyrins **H_2P1**, **H_2P2** and **H_2P3** and also to the metalloporphyrins **FeP1** and **FeP2**, being completely insoluble in all the solvents tested, including those where both **FeP1** and **FeP2** were soluble or partially soluble (DMF, acetone or THF).

The UV-Vis spectrum of the solid **FeP3S** obtained in a dispersion solution of mineral oil (Nujol mull) displayed a broad Soret band at 426 nm, which was red-shifted (*ca.* 13 nm) in comparison to the Soret band at 413 nm of the **H_2P3** precursor, obtained under similar conditions (mineral oil) (Figure 1). The broadening and the red-shift observed for the Soret band (*ca.*

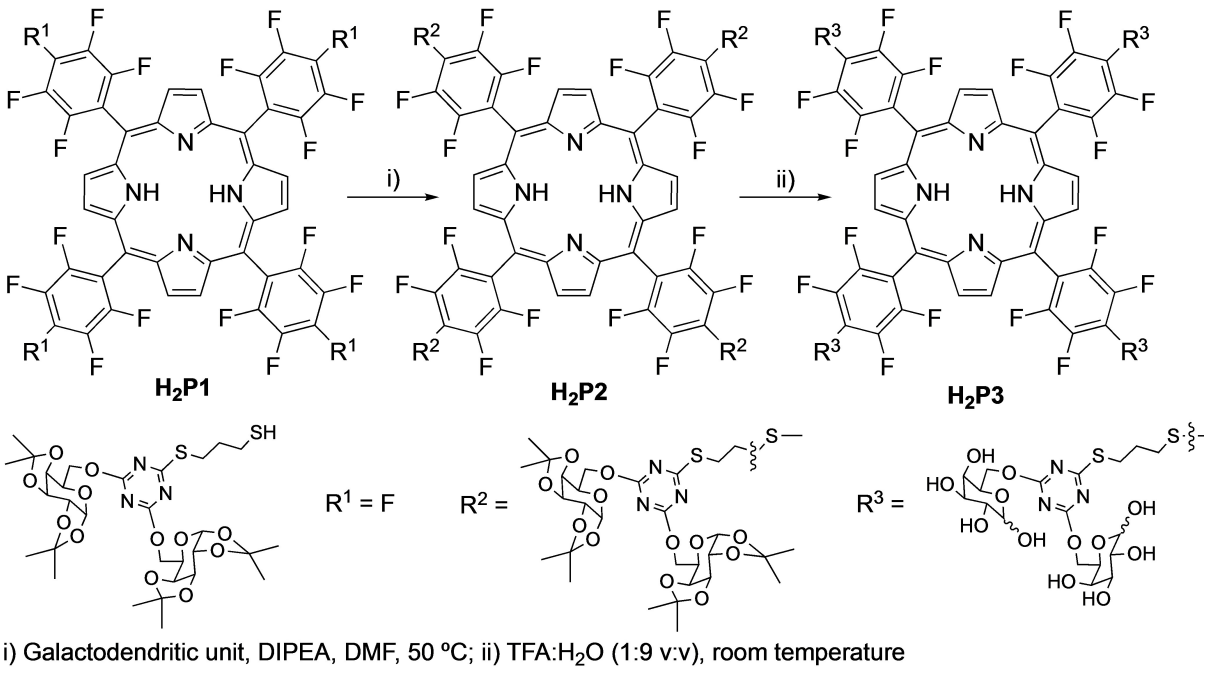

Scheme 1. Schematic representation of the synthetic methodology used in the preparation of the free-base galactodendritic porphyrins **H_2P2** and **H_2P3** from the scaffold **H_2P1**.

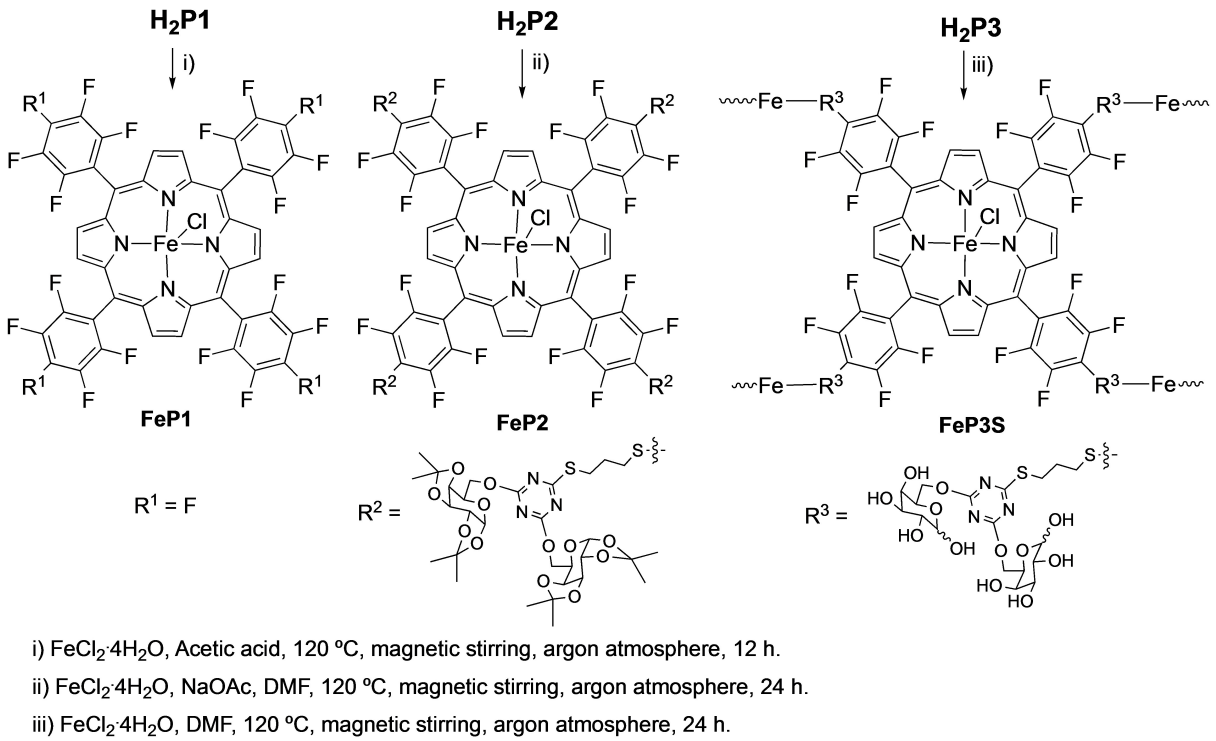

Scheme 2. Schematic synthetic methodology used in the preparation of the iron(III) porphyrins **FeP1**, **FeP2** and **FeP3S**.

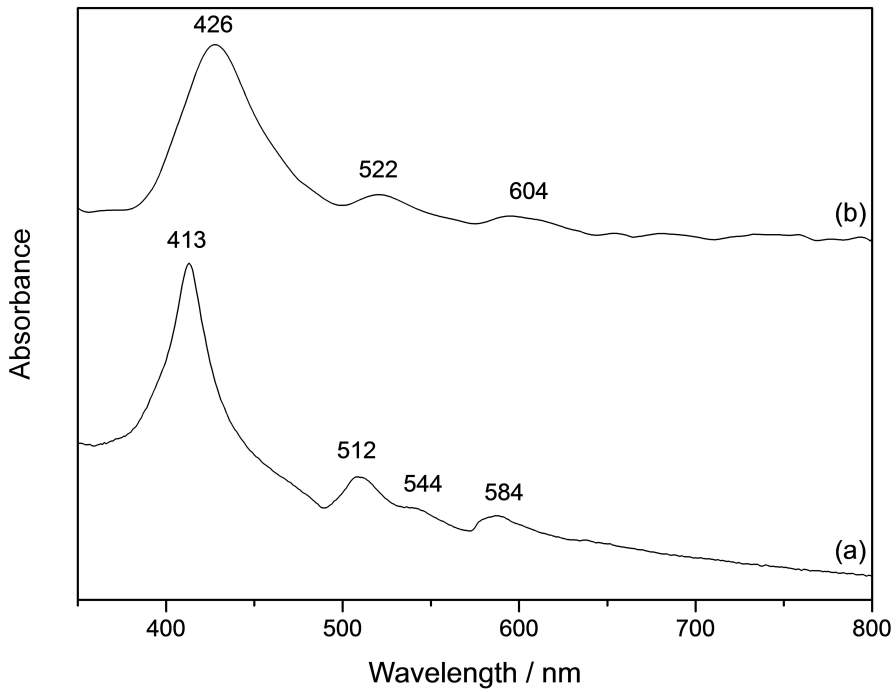

Figure 1. UV-Vis spectra of the solid samples dispersed in Nujol mull: (a) **H_2P3** and (b) **FeP3S**.

13 nm) seem to indicate that significant distortion in porphyrin conformation occurred, which can be related to modifications in the aromatic arrangement affecting the porphyrin ring symmetry.[3g,17a] The spectrum pattern in the visible region with changes in the number and position of Q-bands confirmed that the metalation process occurred.[17b] The insolubility in conventional solvents and the presence of the metalloporphyrins characteristic bands in the electronic spectrum of **FeP3S**

suggest that the metalation of **H_2P3** under the experimental conditions used may have resulted in the formation of this insoluble solid due to the binding of the unprotected glycodendrimers (R^3), the substituents present in the macrocycle, and the metal ion used in excess for the metalation process.

This behavior was not observed for **FeP2** since the galactose units possess isopropylidene protective groups (R^2), which hinder the formation of a structured solid network. The ability of galactose dendrimer units (R^3) to form an insoluble structured solid as a coordination polymer was already reported by us using the same porphyrin with sugar dendrimer (**H_2P3**) in a self-assembly reaction using an excess of copper(II) acetate salt.[3g] Moreover, it was reported that the presence of dendrimers as substituents in different compounds are able to form supramolecular structures by self-assembly[18] and these structures result in insoluble solids.

Mostafa and co-workers reported the coordination of iron(III) with sugar-type ligands (including sugar acids, di- and tri-saccharides).[19] The ligands contains one, two, three or four deprotonated hydroxyl groups that are coordinated to iron(III). The presence of iron(III) species was identified by EPR analyses.[19] The metal complexation by saccharides and derivatives were also reported by Rao and co-workers[20] and Yano and co-workers.[21] For some iron(III) complexes, the coordination of saccharides occurs through the oxygens of the hydroxyl ligands, including the deprotonated hydroxyl groups.[20b]

The ATR-FTIR spectra of the **H_2P2** and **H_2P3** exhibit the typical bands of the macrocycle skeletal ring (Figure 2), as previously reported.[3g] The **FeP2** spectrum (Figure 2e) displays the characteristic bands of porphyrin **H_2P2** (Figure 2b). The disappearance of the bands in the 3300 cm^{-1} region, relative to N–H stretching, and in the 1600 cm^{-1} region, related to δ*N*-H vibration of the pyrrole ring in the spectrum of **FeP2**, indicates the presence of iron ion in the core of the macrocycle,[3c] as observed in the spectrum of **FeP1**.[3f] The band at 1727 cm^{-1} may be due to the C=O stretching from DMF used as solvent in the preparation of **FeP2** in comparison to the spectrum observed for **FeP1**.[22] The spectrum of the solid **FeP3S** resembles the spectrum of porphyrin **H_2P3** (Figure 2f and Figure 2c, respectively). In both spectra, the bands at 3400 cm^{-1} (O–H stretching, broad) and 667 cm^{-1} (C–N stretching) are assigned to the glycodendritic moieties.[3c] The presence of an extremely broad band in the 3500 cm^{-1} region in both spectra ends up overlapping the region of 3300 cm^{-1}, characteristic of the *N*–H stretching, which is one of the main bands to confirm if the metal ion was inserted into the macrocycle core or if it still remains as a free-base porphyrin. However, the disappearance of a broad band in the region of 1600 cm^{-1}, related to δN–H vibration of the pyrrole ring in the **FeP3S** spectrum, when compared to **H_2P3**, seems to corroborate the metalation of the inner core of the macrocycle. In addition, for the **H_2P3**, the broad band at 1655 cm^{-1} can also be attributed to triazine ring. The disappearance of this band and the concomitant presence of two bands at 850 and 890 cm^{-1} indicate the presence of metal-saccharide portions in the **FeP3S** spectrum.[20a] The disappearance of a band of triazine group also suggests some interaction with N atoms as reported by Huang and co-workers for the CAU-7-TATB framework structure.[23] The band at 1592 cm^{-1} probably is due the

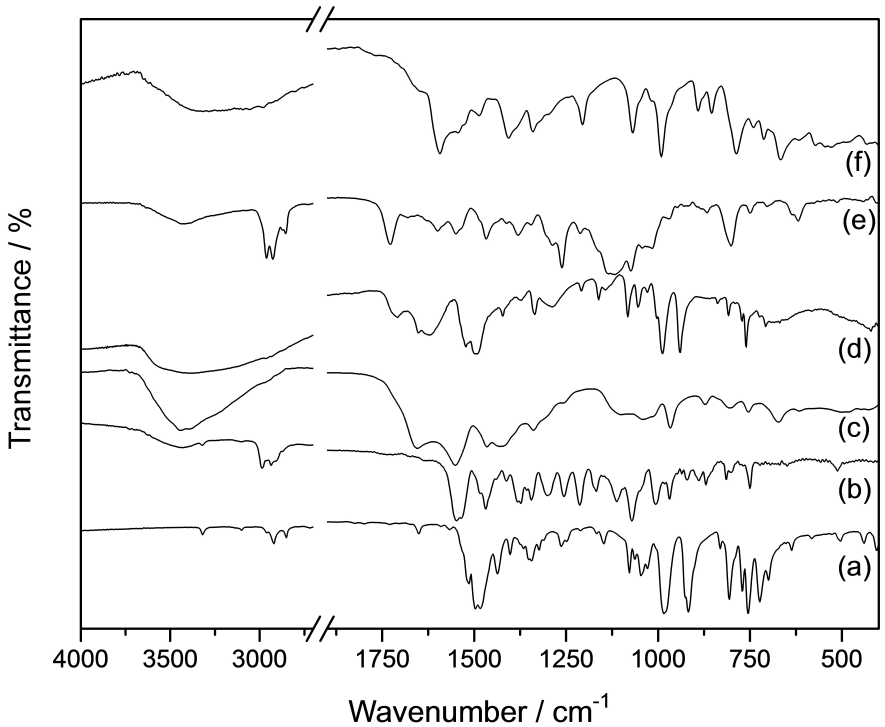

Figure 2. ATR-FTIR spectra of the free-base porphyrins and the iron(III) porphyrins: free-base porphyrins (a) **H_2P1**, (b) **H_2P2**, and (c) **H_2P3**; iron(III) porphyrins (d) **FeP1**, (e) **FeP2**, and (f) **FeP3S** (the 2750–2050 cm^{-1} region was omitted, due to the absence of bands).

bending vibrations of H_2O or the possible open form of dendrimer group.[20a]

The EPR spectrum recorded for the **FeP1** solid sample at 77 K (Figure 3) displays the characteristic signals of high-spin Fe^{3+} (S = 5/2) in axial symmetry with signals in the region of $g_{\perp} = 6.0$ and $g_{//} = 2.0$. According to the literature,[24] transitions relative to the Kramer doublet $\pm 1/2$ ($g_{\perp} = 6.0$ and $g_{\parallel} = 2.0$) are observed in the spectra of EPR when high-spin Fe^{3+} is found in a tetragonal symmetry. In a less symmetrical environment, such as orthorhombic symmetry, the appearance of additional signs with values of g = 4.3 are observed.[3c] Interestingly, **FeP2** and **FeP3S** evidence not only a low-intensity signal at g = 6.0 but also show a signal at g = 4.3, characteristic of high-spin iron(III) in rhombic symmetry, indicating that the insertion of the sugar dendrimers (R^2 for **FeP2** and R^3 for **FeP3S**, Scheme 2) causes distortions in the porphyrin ring which leads to the presence of iron ions in an environment of lower symmetry. A rather intense signal centered at g = 2.0 is also observed in both spectra, being highly unsymmetrical and broad for **FeP3S**. It is reported in the literature[25] that high-spin iron(III) complexes with sugar-type ligands, such as galactose, sorbitol or 1,2-propylene glycol, show a broad signal around g = 2.0 attributed to Fe^{3+} in octahedral surroundings. The EPR result (Figure 3b) may suggest that some iron(III) ions used in the metalation of the ligand **H_2P2** can be coordinated to the sugar dendrimers (R^2 groups) in **FeP2**. In the EPR spectrum of **FeP3S** (Figure 3c) a broad signal at g = 2.0 is observed and this broadening of the signal in comparison to the signal observed for **FeP2** (Figure 3b) can be related to iron-iron coupling with a resonance absorption at g = 2.0 due to spin-spin interaction, as reported in the literature,[26] suggesting the formation of an iron complex network in a structured solid. Naik and co-workers,[26c] for example, reported a similar iron(III) EPR behavior for Fe^{3+} doped Mg_2SiO_4 nanomaterials, where samples with higher concentration of iron(III) presented higher intensity for the broad signal at g = 2.0. Iron(III)-saccharide complexes (mono and bi-nuclear) were reported by Rao and co-workers,[20b] all the iron(III) complexes exhibited two signals characteristic of iron(III), a sharp signal at g ~ 4.2 and a broad signal at g = 2.0 caused by the coordination of hydroxyl groups and deprotonated hydroxyl groups. Similar spectra EPR were reported for iron(III) complexes of D-glucose and D-fructose[27] and other sugar type ligands coordinated to iron(III).[19]

Catalytic studies

The catalytic activity of **FeP1** in solution (homogeneous catalysis) is well established in the literature[24a,b,28] and in our group.[3c,f,g] These studies show that **FeP1** usually presents high yields for the production of different epoxides in olefins epoxidation, and also shows selectivity for the formation of alcohols when inert alkanes are used as substrates, *e.g.* cyclohexane to cyclohexanol[3c,f] and heptane to several heptanols.[3f] Based on the catalytic activity of **FeP1** and on all the studies over the last few years showing that porphyrins containing electronegative and/or bulky substituents at the *meso* position of the macrocycle are more robust and very suitable catalysts in (ep)oxidation reactions,[13a,c] the catalytic assays with the iron(III) porphyrins **FeP2** (homogeneous catalysis) and **FeP3S** (heterogeneous catalysis) were explored in order to study the influence of R^2 and R^3 groups and the possible structured solid resulted by it, in the catalytic results of these classes of catalysts.

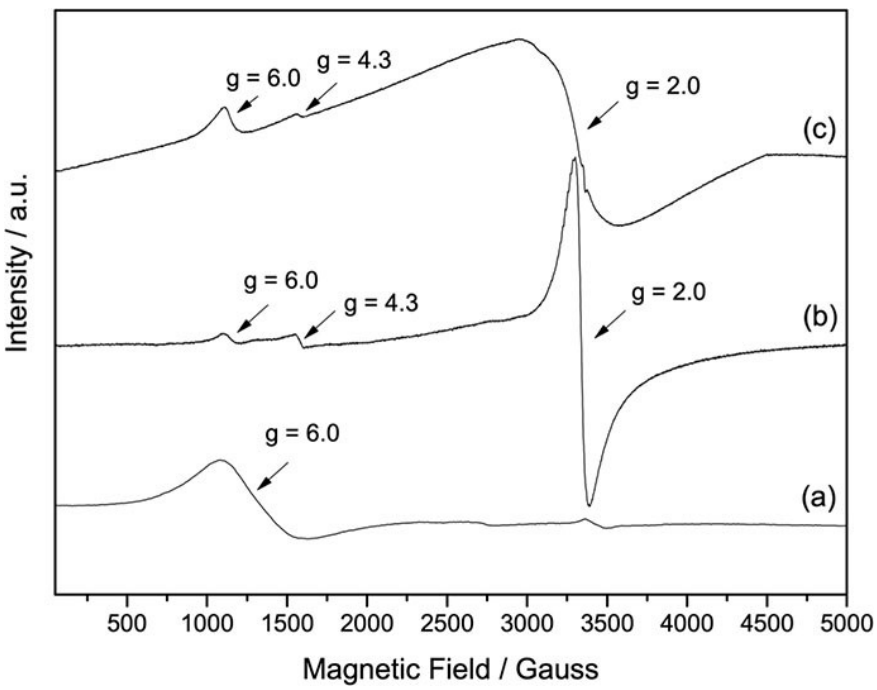

Figure 3. EPR spectra recorded for solid samples at 77 K: (a) **FeP1**, (b) **FeP2** and (c) **FeP3S**.

(Z)-Cyclooctene

The ability of metalloporphyrins to efficiently epoxidize (*Z*)-cyclooctene, leading to a single product, cyclooctene oxide, makes this alkene an excellent diagnostic substrate to evaluate the catalytic efficiency of such catalysts.[3g,h,29] It has been established that bulky and/or electronegative groups or elements at the *ortho* positions of the *meso* aryl substituents of the porphyrin macrocycle can contribute to generate and stabilize the active catalytic species.[11d,13] These electronegative substituents can prevent porphyrin destruction by self-interaction in solution and lead to efficient and selective catalysts for oxidation reactions. Thus, as previously reported by us, the excellent catalytic activity observed for **FeP1** was not surprising (100% epoxide yield, Figure 4).[3f] This is due to the electron-withdrawing pentafluorophenyl substituents at the *meso* position of this porphyrin macrocycle, contributing to the electronic density reduction on the macrocycle, thereby stabilizing the catalyst against oxidative degradation.[13a,c] However, the catalytic efficiency of the homogeneous complex **FeP2** under the same conditions (Figure 4) shows a significant decrease (75% epoxide yield) if compared to **FeP1**. These results can be associated with a decrease in the electron-withdrawing effect when one fluorine atom per each *meso*-pentafluorophenyl substituent in **FeP1** (four fluorine atoms in total) is substituted by the galactose dendrimer unit in **FeP2**. In this case, the presence of electronegative substituents seems to be more effective than bulky substituents when better catalytic activity is sought.[3g,14a,30]

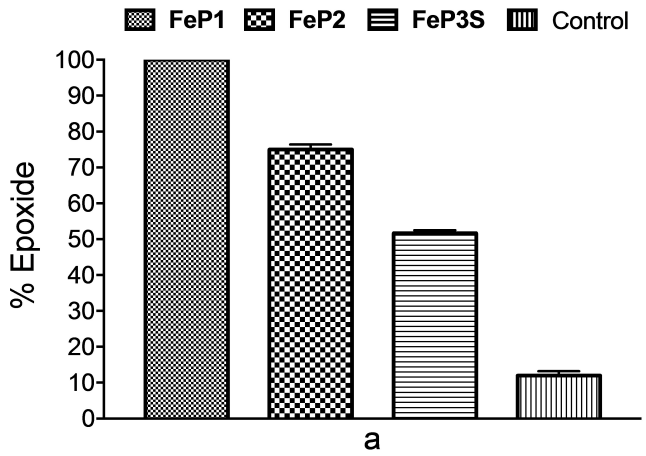

Figure 4. Oxidation of (*Z*)-cyclooctene by PhIO using **FeP1**, **FeP2** or **FeP3S** as catalysts. [a]Reaction conditions: reaction time 1 h, **FePx**/PhIO/substrate molar ratio = 1:50:5000. All reactions were performed at least in duplicate using acetonitrile. The percentage yield was calculated based on the amount of PhIO. The result for **FeP1** is from reference.[3f] Control = reactions performed in the presence of PhIO and in the absence of any catalyst, using the same conditions described above.

The heterogeneous catalysis using the solid **FeP3S** shows, under the same conditions (Figure 4), a more pronounced decay in catalytic activity (epoxide yield around 52%) in comparison to **FeP1**. This can be explained by (i) the decrease in the electron-withdrawing effect, caused by the substitution of four fluorine groups by R^3, as well as in **FeP2**, and (ii) the insolubility of the catalyst in the reaction medium. This insolubility can limit the access of PhIO to some of the metal sites in the bulk solid **FeP3S** to form the active catalytic species, and also the access of the substrate to these active catalytic species. In this new scenario, where the catalyst is a bulky solid, probably only the iron at the surface of the insoluble particles of the solid is accessible to PhIO and to the substrate. In fact, by changing the solvent of the reaction, from pure acetonitrile (Figure 5a) that was used to promote a better solubility of PhIO, to an acetonitrile/dichloromethane (ACN/DCM) mixture, where the substrate is more soluble (Figure 5b), no yield changes were registered, showing how the insolubility of the **FeP3S** catalyst is a key feature in the epoxide yield decrease observed (Figure 5). However, an extension of the reaction time from 1 h to 24 h resulted in an improvement in the epoxide yield from around 52% to 65%, for the reaction in acetonitrile (Figure 5c). This result shows that extending the reaction time can favor the

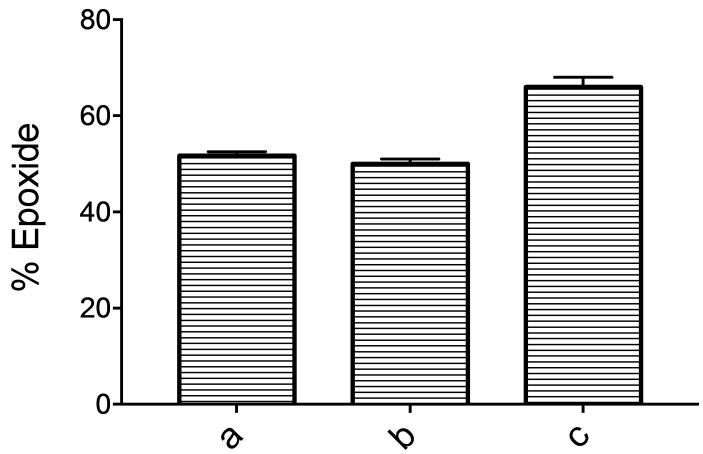

Figure 5. Oxidation of (*Z*)-cyclooctene by PhIO using **FeP3S** as catalyst. Reaction conditions: **FeP3S**/PhIO/substrate molar ratio = 1:50:5000. All reactions were performed at least in duplicate using a) reaction time 1 h, in acetonitrile or b) reaction time 1 h, in acetonitrile/dichloromethane (1:1 v:v) as solvent; c) reaction time 24 h, in acetonitrile as solvent. The yields were calculated based on the amount of PhIO.

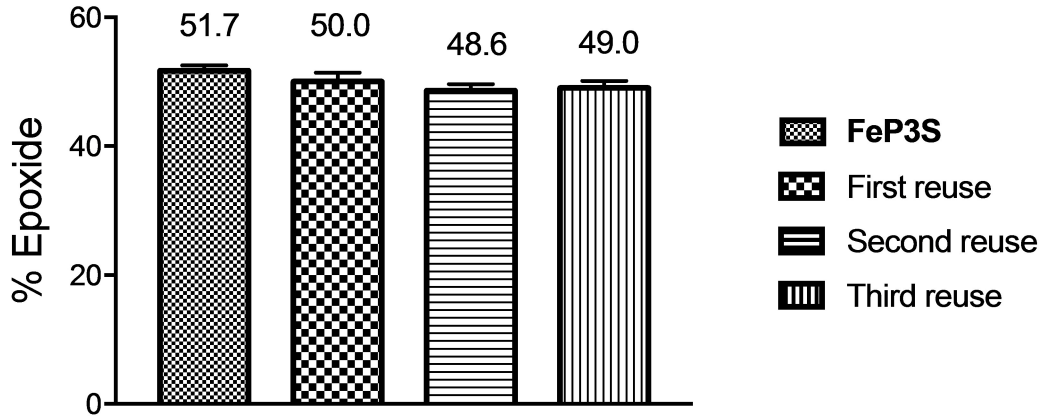

Figure 6. Oxidation of (Z)-cyclooctene by PhIO using **FeP3S** as catalyst. Reaction conditions: reaction time 1 h; **FeP3S**/PhIO/substrate molar ratio = 1:50:5000; all reactions were performed at least in duplicate, using acetonitrile as solvent. The yields were calculated based on the amount of PhIO.

yield, since the access of all the reactants to the porphyrin metal center is favored, either by promoting the formation of the active catalytic species by the interaction of the porphyrin metal center with PhIO, or by promoting the access of the substrate to the active catalytic species formed.

On the other hand, the insolubility of **FeP3S** can be an advantage in this catalytic system because it allows the recovery of the catalyst by centrifugation, separation, purification and reuse of the solid in more than one catalytic run. It was possible to efficiently recover and recycle **FeP3S** at least three times without significant mass loss and a decrease in catalyst activity. The results are summarized in Figure 6 and show that the epoxide yields obtained in the consecutive runs are similar to the first use. These results show that the solid catalyst (**FeP3S**) is stable and remains active after the first use, being resistant to the reaction conditions and the various washing and drying processes used for its activation.

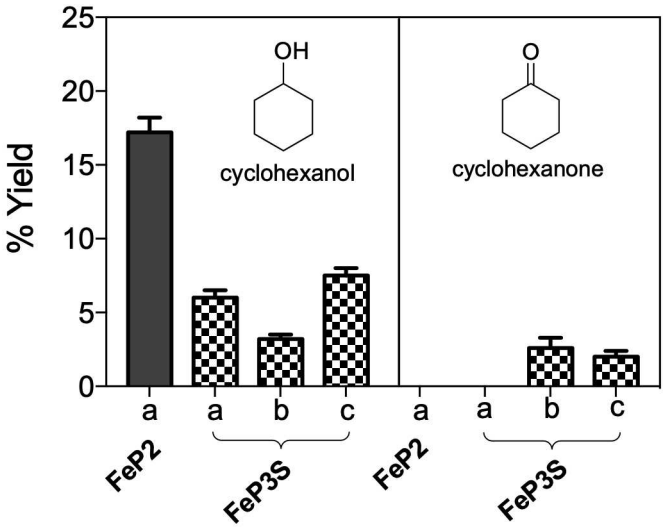

Figure 7. Oxidation of cyclohexane by PhIO using **FeP2** and **FeP3S** as catalysts. Reaction conditions: **FePx**/PhIO/substrate molar ratio = 1:50:5000. All reactions were performed at least in duplicate. a) Reaction time 1 h; acetonitrile as solvent. b) Reaction time 1 h; acetonitrile/dichloromethane (1:1 v/v) as solvent; c) reaction time 24 h; acetonitrile as solvent. For all the reaction and conditions studied the products' yields (cyclohexanol and cyclohexanone) were calculated based on the amount of PhIO.

Cyclohexane

Cyclohexane is a less reactive substrate in oxidation reactions in comparison to cyclooctene previously investigated. This is not a problem in catalysis using metalloporphyrins, since this allows to investigate the catalytic efficiency and selectivity of the catalytic species once cyclohexanol and cyclohexanone are major products in metalloporphyrins catalyzed oxidation reactions using PhIO as oxidant.[3e,l,31] In general, oxidation reactions catalyzed by metalloporphyrins, contrarily to other catalysts,[32] are selective for the alcohol showing the versatility of this class of complexes as catalysts.[3i,11d] This selectivity is directly related to the reaction mechanism,[3e] where the cyclohexyl radical is kept close to the high valent hydroxo-metallo(IV)porphyrin (M^{IV}(OH)P) intermediate by the formation of a solvent cage. Usually, this solvent is long-lived enough to allow a transfer of a hydroxyl group from the M^{IV}(OH)P intermediate to the organic radical, leading to the preferential formation of cyclohexanol.

Figure 7 shows the results obtained for the oxidation of cyclohexane using **FeP2** and **FeP3S** as catalysts. The results obtained in cyclohexane oxidation by **FeP1** were previously reported by our group,[3c,f] where this catalyst shows high efficiency (alcohol + ketone total yield 87%) and selectivity for cyclohexanol (98%) in comparison to cyclohexanone.

Using **FeP2** as catalyst, 17% alcohol yield was observed in the oxidation of cyclohexane in acetonitrile, with no production of cyclohexanone (100% alcohol selectivity) under the same reaction conditions as for **FeP1** (Figure 7).[3c] As discussed previously for the epoxidation of (*Z*)-cyclooctene, the substitution of the fluorine atoms by the bulky dendrimer units may justify the products' yield decrease,[3c] the influence of this substitution on the catalytic results being even more dramatic when the oxidation of a more inert substrate, such as cyclohexane, is explored.

Regarding the use of **FeP3S** under heterogeneous conditions, a pronounced decay is observed for cyclohexanol yield in different experimental conditions [acetonitrile as solvent, after 1 h of reaction (Figure 7a); ACN/DCM mixture (1:1) as solvent, after 1 h of reaction (Figure 7b), and acetonitrile as solvent, after 24 h of reaction (Figure 7c)] in comparison to the cyclohexanol yield observed for **FeP2** under homogeneous conditions (Figure 7a). However, despite the well-known cyclohexane inertia in oxidation reactions, this insoluble solid catalyst also presents catalytic activity.

Using **FeP3S** as catalyst a cyclohexanone yield increase may occur, depending on the experimental conditions chosen. For example, using a less polar reaction solvent (a mixture of ACN/DCM, Figure 7b) the alcohol yield is similar to the ketone yield, decreasing the selectivity of the reaction for cyclohexanol. When the reaction time increases to 24 h (Figure 7c), the alcohol yield increases in comparison to 1 h reaction in acetonitrile (Figure 7a), while lowering the selectivity for cyclohexanol because cyclohexanone is also formed. During the 24 h reaction in acetonitrile (Figure 7c), the alcohol produced probably undergo catalytic overoxidation into the ketone. The catalytic results observed in Figure 7 suggest that **FeP3S** can be structured in a system of channels and pores that probably favors the permanence of the alcohol near the active sites of the solid catalyst, thus promoting its overoxidation if the reaction is prolonged for 24 hours. This possibility of a hierarchical system of pores in the solid **FeP3S** motivated the investigation of its catalytic activity using a linear alkane, capable of accessing the pores and channels of this hypothetical porous system.

Heptane

Linear alkanes are among the most difficult organic molecules to be oxidized due to the chemical inertia of the C–H and C–C single bonds.[33] In addition, another challenge in the oxo-functionalization of these compounds is related to regioselectivity, since the energy of dissociation of C–H bonds in linear alkanes becomes greater as the carbon is less substituted, as can be seen for tertiary (96.5 kcal/mol), secondary (98.6 kcal/mol) and primary (101.1 kcal/mol) carbons.[9,34] In this way, the oxidation of the heptane, for example, preferentially produces heptan-2-ol and heptan-3-ol due to both energetic and statistical factors.[3f,35] Thus, for this substrate the yield of the hydroxylation products usually follows the order heptan-3-ol ~ heptan-2-ol > heptan-4-ol ≫ heptan-1-ol, independent of the catalyst used.[3f,35a] On the other hand, products from the oxidation of linear alkanes in the terminal positions are of great interest for the chemical and pharmaceutical industry since, for example, they can be used for the production of adipic acid, from the oxidation of hexane in terminal positions, an important commodity for the production of Nylon-6,6.[8,36] Synthetic metalloporphyrins have been intensely studied as catalysts in the oxo-functionalization of these less reactive substrates in the attempt to obtain more efficient and environmentally friendly selective catalytic systems.[11c,37]

The results obtained for the oxidation of heptane in homogeneous (**FeP1** and **FeP2**) and heterogeneous (**FeP3S**) conditions are presented in Figure 8 and Figure 9. In all cases and reaction conditions, as well as in the hydroxylation of cyclohexane (Figure 7), higher selectivity for the alcohol products is observed, as expected when using metalloporphyrins as catalysts.[11c,37a,38]

As previously reported by us,[3f] the homogeneous catalyst **FeP1** afforded good global yield for the alcohols (~34%) after 1 h of reaction in acetonitrile, showing high alcohol selectivity (alcohol/ketone ratio ~17) with high yield for 2-ol and 3-ol alcohol products, and regioselectivity of 3-ol ~ 2-ol > 4-ol ≫ 1-ol (Figure 8a). Moreover, when using the ACN/DCM mixture as solvent for **FeP1** (after 1 h of reaction, Figure 8b) or when the reaction time was increased for the same catalyst (from 1 h to 24 h in acetonitrile, Figure 9a) the alcohols' total yield did not change, remaining around 36%, always favoring oxidation at positions 2 and 3 relatively to positions 4 and 1 in heptane (alcohols' regioselectivity after 24 h in acetonitrile and after 1 h of reaction in ACN/DCM mixture: 2-ol ~ 3-ol > 4-ol ≫ 1-ol).

On the other hand, for the reactions using **FeP2** as catalyst, both in acetonitrile or ACN/DCM mixture (Figure 8), total selectivity for the alcohols is registered, since no ketones are formed, but a decrease of alcohols' global yield is observed (18–19%), similarly to the results obtained with **FeP1** and **FeP2** for cyclohexane, as discussed before. Both catalysts present a similar tendency concerning regioselectivity, the higher alcohol yields being registered at C2 and C3 after 1 h of reaction (**FeP2**, Figure 8). **FeP2** and **FeP1** evidence also a similar behavior when the solvent is changed (Figure 8a,b). Both catalysts give rise to better alcohol yields after 1 h if the ACN/DCM mixture is used as solvent.

In order to further investigate the regioselectivity in the oxidation of heptane with **FeP2** as catalyst, the reaction time was extended to 24 h, both in acetonitrile (**FeP2**, Figure 9a) and in ACN/DCM mixture (**FeP2**, Figure 9b).

A very interesting result was observed for this catalyst **FeP2** in acetonitrile, where the formation of alcohols is favored (29.5% after 24 h, Figure 9a *vs* 18.2% after 1 h, Figure 8a), notably with higher yield for heptan-1-ol (~10%). Besides, an inversion in regioselectivity was also observed, specifically 1-ol > 2-ol > 3-ol ≫ 4-ol (after 24 h in ACN) *vs* 2-ol ~ 3-ol > 4-ol > 1-ol (after 1 h in ACN). These results are in agreement with the literature,[14b,39] which indicates that metalloporphyrins with bulky substituents can promote the reaction at the terminal positions of linear alkanes due to the restriction access of the other carbon positions of the substrate to the metal center. Thu and co-workers[40] demonstrated that the use of highly sterically demanding rhodium-porphyrin catalysts led to selective carbene insertion into a primary C–H bond, with remarkably high selectivity (>80%) in the reactions with hexane, octane and decane, for example. Rebouças and co-workers[41] reported the oxidation of heptane using a series of neutral and cationic manganese(III) porphyrins (MnPs) as catalysts and PhIO as oxidant. In this study, the authors observed an inversion in heptane oxidation chemoselectivity after immobilization on the Sil–Cl support if compared to the MnP in solution. The non-immobilized MnPs showed chemoselectivity toward the

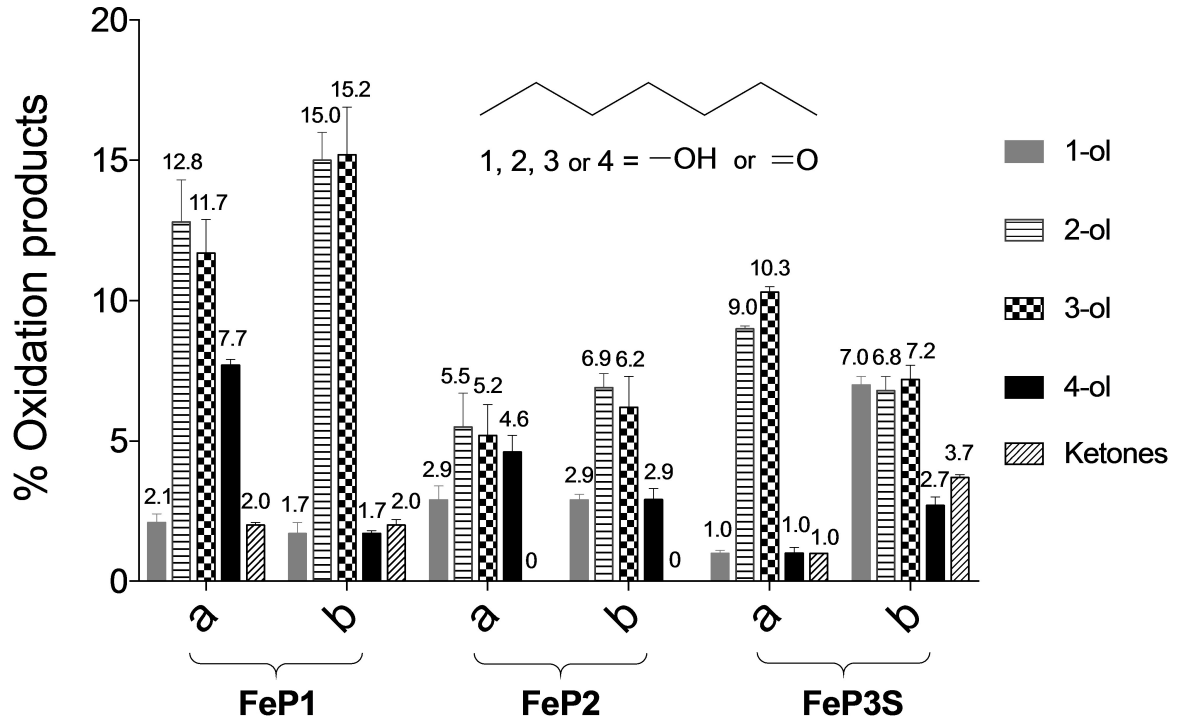

Figure 8. Oxidation of heptane by PhIO using **FeP1**, **FeP2** or **FeP3S** as catalysts. Reaction conditions: **FePx**/PhIO/substrate molar ratio = 1:50:5000; reaction time 1 h; all reactions were performed at least in duplicate using (a) acetonitrile or (b) acetonitrile/dichloromethane (1:1 v:v) as solvent. The yields were calculated based on the amount of PhIO. Alcohol products: 4-ol = heptan-4-ol; 3-ol = heptan-3-ol; 2-ol = heptan-2-ol, and 1-ol = heptan-1-ol. Ketone products: heptan-2-one + heptan-3-one + heptan-4-one.

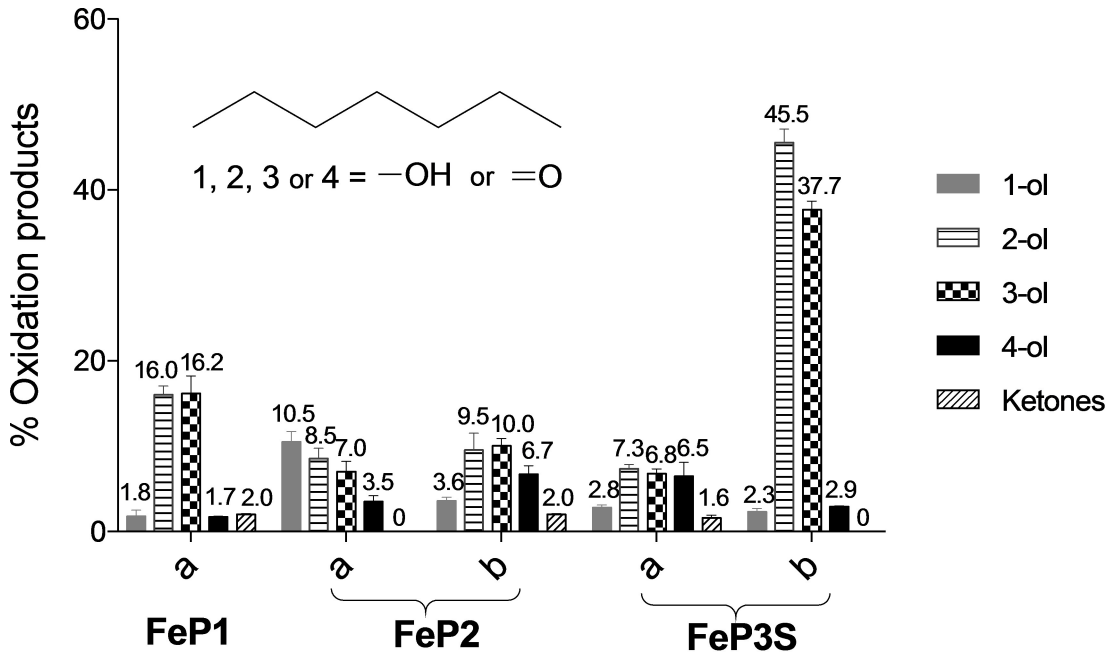

Figure 9. Oxidation of heptane by PhIO using **FeP1**, **FeP2** or **FeP3S** as catalysts. Reaction conditions: **FePx**/PhIO/substrate molar ratio = 1/50/5000; reaction time 24 h; all reactions were performed at least in duplicate using (a) acetonitrile or (b) acetonitrile/dichloromethane (1:1 v:v) as solvent. The yields were calculated based on the amount of PhIO. Alcohol products: 4-ol = heptan-4-ol; 3-ol = heptan-3-ol; 2-ol = heptan-2-ol, and 1-ol = heptan-1-ol; Ketones products = heptan-2-one + heptan-3-one + heptan-4-one.

carbonyl products. Comparing the results obtained here for the **FePs** with those reported by Rebouças and co-workers[41] for the non-immobilized MnPs, the alcohol global yield are higher, though depending on the solvent used.

For the reactions carried out in the ACN/DCM mixture for 24 h (Figure 9b), **FeP2** gives an alcohols' total yield higher than for 1 h (~19% after 1 h, Figure 8b *vs* ~30% after 24 h, Figure 9b), the regioselectivity of the reaction being similar to that observed in acetonitrile after 1 h of reaction (2-ol ~ 3-ol > 4-ol ⩾ 1-ol). Furthermore, **FeP2** affords total selectivity for the alcohols from heptane oxidation in three of the four reaction conditions evaluated: (i) acetonitrile as solvent after 1 h of reaction; (ii) ACN/DCM mixture as solvent after 1 h of reaction; acetonitrile as solvent after 24 h of reaction. However, when the mixture of ACN/DCM was used and the reaction was left for 24 h, 2% yield for ketones were detected, so the alcohols' selectivity was reduced to 94% approximately (Figure 9b).

The solid catalyst **FeP3S** (Figures 8 and 9) presented some very interesting results compared to **FeP2**. Using similar experimental conditions (after 1 h of reaction, Figure 8a or after 24 h of reaction, Figure 9a), the solid catalyst **FeP3S** gave rise to similar alcohols' global yields if compared to the homogeneous **FeP2**, in acetonitrile, for the same reaction time. For example, after 1 h of reaction (Figure 8a) ~21% alcohols' global yield for **FeP3S** *vs* ~19% for **FeP2** were obtained. In contrast, after 24 h of reaction (Figure 9a) ~23% alcohols' global yield for **FeP3S** *vs* 29.5% for **FeP2** were achieved, in acetonitrile as solvent.

Mansuy and co-workers[38,42] studied the oxidation of adamantane, heptane, and pentane in the presence of cationic manganese(III) porphyrins immobilized on montmorillonite clay. The regioselectivity observed was the same as reported for the same porphyrin but immobilized on silica.[43] For example, for the heptanols' global yield up to 40% were obtained (3-ol ~ 2-ol ⩾ 4-ol). Comparing to the results obtained here, at the same reaction time, the alcohols' global yield reported by Mansuy and co-workers[42] was higher. Differently, here we observe the oxidation at C1 (7% of heptan-1-ol in ACN/DCM mixture for **FeP3S**, Figure 8b); moreover, it is clear that **FeP3S** exhibits better catalytic performance when increasing the reaction time (Figure 9b).

When the manganese porphyrinosilicas[37a] obtained from the reaction of **FeP1** with 3-aminopropyltriethoxisilane (3-APTS) were used as catalysts for heptane oxidation, as reported by Battioni and co-workers, a similar global yield (*ca* 45%) to that described by Mansuy[42] was observed, although with a longer reaction time (24 h).

The heterogeneous or homogeneous character of the catalytic process can also affect regioselectivity.[41] In acetonitrile as solvent and after 1 h of reaction (Figure 8a), the regioselectivity is quite similar in both cases: 2-ol ~ 3-ol > 4-ol > 1-ol for **FeP2** and 2-ol ~ 3-ol > 4-ol ~ 1-ol for **FeP3S**. However, when the reaction in acetonitrile was left for 24 h (Figure 9a), the **FeP3S** (a heterogeneous process) gave rise to heptan-2-ol (7.3%), heptan-3-ol (6.8%) and heptan-4-ol (6.5%) in similar proportions, and only a small increase of approximately 0.6% of ketones occurred. This result differs from the regioselectivity observed for **FeP2**, that under similar conditions, an increase in heptan-1-ol was observed. The inversion of regioselectivity observed for **FeP3S** in comparison to **FeP2** can be attributed to an easier permeation of the substrate inside the putative pores presented by **FeP3S**, as already suspected for the catalytic results using cyclohexane. A longer contact time between the catalyst species and the substrate, considering the substrate can permeate in the solid catalyst **Fe3PS** by the pore and channel system, can facilitate the interactions between species promoting catalysis, as a consequence the formation of the favorable products, *e.g.* heptan-2-ol, heptan-3-ol and heptan-4-ol, was observed. These results suggest that the porous systems supposed for **FeP3S** can affect the way the substrate interacts with the catalytic species present thus imposing the observed selectivity.

Suslick and co-workers[14b] demonstrated, under heterogeneous catalytic conditions using a microporous porphyrinic solid, that more robust frameworks with the presence of channels or pores with appropriated size may favor the oxidation of energetic or statistically less favorable positions in linear alkanes. The solid catalyst PIZA-3 [(Mn(T*p*CPP)$Mn_{1.5}$)$(C_3H_7NO)\cdot 5(C_3H_7NO)$] used by Suslick and co-workers for the heptane oxidation in acetonitrile (reaction conditions: catalyst/oxidant/substrate/imidazole molar ratio 1 : 10 : 1000 : 1, for 2 h at room temperature) showed an alcohols' global yield of 23% [heptan-2-ol (8%), heptan-3-ol (10%) and heptan-4-ol (5%)].

In the ACN/DCM mixture and changing the time from 1 h to 24 h, the alcohols' global yield for **FeP2** showed a modest increase (~19% to ~30%) (Figure 8b and Figure 9b). However, for **FeP3S** this mixture of solvents causes a high efficiency of the catalyst, affording ~88% of alcohols' global yield after 24 h instead of ~24% after 1 h (Figure 9b and Figure 8b, respectively). These values are much higher than those observed for the homogeneous catalysts (**FeP1** and **FeP2**). Moreover, the increase in reaction time tends to oxidize the most energetically and statistically favored positions, 3-ol (~38%) and 2-ol (~45%) in relation to 4-ol (~3%) and 1-ol (~2%). These results indicate that, under these conditions, the pores of **FeP3S** solid may be clogged over time, and catalysis may occur on the surface of the material, leading to an increased oxidation rate at C2 and C3. These results are comparable to those reported by Mansuy and co-workers using iron(III) perhalogenated porphyrins in solution (up to *ca* 80%). Considering these results, the authors concluded that chemoselectivity and regioselectivity vary depending on the presence or absence of halogens.[44]

The results found in this work suggest that the adequate choice of solvent and time of reaction can modulate the regioselectivity of the catalyst, due to the effect dendrimeric substituents can impose to the catalytic structure of the obtained solid material, leading to oxidation of difficult-to-oxidize substrates, as linear alkanes such as heptane.

Experimental

All chemicals used in this study were purchased from Sigma Aldrich, or Merck and were of analytical grade. Iodosylbenzene (PhIO) was synthesized by hydrolysis of iodosylbenzenediacetate.[45] The solid PhIO was carefully dried under reduced pressure, kept at 5 °C, and its purity was assessed by iodometric titration.[45–46]

Synthesis of the free-base porphyrins H_2P1, H_2P2, and H_2P3

The free-base porphyrins (**H_2P1**, **H_2P2**, and **H_2P3** were synthesized and characterized by ^{1}H, ^{13}C and ^{19}F NMR, FTIR, mass spectrometry and UV-Vis as previously described in the literature (Scheme 1).[15]

Synthesis of the iron(III) porphyrins FeP1 and FeP2

The metalloporphyrin **FeP1** was synthesized and purified as described in the literature (Scheme 2).[3f] The complex **FeP2** was obtained from metalation of the respective free-base porphyrin **H_2P2** using the modified Kobayashi method.[2l,47] The reaction was performed in *N*,*N*-dimethylformamide (DMF) as solvent, using a 10-fold excess of iron(II) chloride tetrahydrate and sodium acetate (to minimize the protonation of the porphyrin inner core nitrogen atoms) under magnetic stirring at 120 °C and argon atmosphere for 24 h (Scheme 2). Afterward, the solvent was removed under reduced pressure. The solid was purified by silica gel column chromatography using dichloromethane as eluent to yield **FeP2** (87%) as a purple dark solid. **FeP1**: UV-Vis λ_{max}, nm (log ε) (THF): 410 (5.29), 506 (4.27) 566 (3.38) and 624 (3.25) **FeP2**: UV-Vis λ_{max}, nm (log ε) (THF): 414 (5.34), 505 (4.16), 584 (3.70) and 648 (3.29).

Synthesis of the material (FeP3S)

The metalation procedure of the free-base porphyrin **H_2P3** with 10 equiv. of iron(II) chloride tetrahydrate took place as shown in Scheme 2, affording, after 24 h, a deep dark purple solid that from now on will be designated as **FeP3S**. That solid product is insoluble in all the solvents tested (DMF, H_2O, acetone, methanol, and THF). The solid was isolated by filtration, washed thoroughly with different solvents (DMF, $CHCl_3$, CH_2Cl_2, CH_3OH, H_2O, and acetone), dried under reduced pressure and then characterized by different techniques (UV-Vis, ATR-FTIR and EPR).

Evaluation of the catalytic activity of the iron(III) porphyrins FeP1, FeP2 and FeP3S in the oxidation of (*Z*)-cyclooctene, cyclohexane and heptane

The oxidation reactions in the presence of the iron(III) porphyrins were carried out in a thermostatic glass reactor equipped with a magnetic stirrer, placed inside a dark chamber. The catalytic studies were done using (*Z*)-cyclooctene (freshly purified by alumina column chromatography),[48] cyclohexane and heptane as substrates, and iodosylbenzene (PhIO) as oxidant. In general, the reactions were performed by purging the glass reactor containing the solid catalyst (**FeP1**, **FeP2** or **FeP3S**) and iodosylbenzene (**FeP**X/PhIO molar ratio 1:50, **X** = **1**, **2** or **3S**) with argon for 15 min. Then, the solid mixture was suspended in 420 μL of solvent (acetonitrile or acetonitrile/dichloromethane (1:1 v/v)) and the adequate substrate (PhIO/substrate molar ratio 1:100) was added; all the oxidation reactions were carried out under an inert atmosphere (Ar) and magnetic stirring at 25 °C for 1 h or 24 h. To finish the reaction, sodium sulfite (acetonitrile saturated solution) was added to the reaction mixture in order to eliminate the excess of PhIO used, and then the solid catalyst was washed with 300 μL of methanol. Finally, the reaction mixture was transferred quantitatively to a volumetric flask. When **FeP3S** was used, the catalyst remained insoluble during all the reaction time (heterogeneous catalysis process). In this case, the reaction mixture, along with the reaction products, were separated from the insoluble catalyst by a centrifugation process and the supernatant was transferred quantitatively to a volumetric flask. The solid catalyst was exhaustively washed with methanol and acetonitrile, in order to extract any reaction products or remaining substrate that might have remained adsorbed onto the catalyst material. The reaction mixtures were analyzed by gas chromatography, using octan-1-ol as internal standard. Product yields were based on the amount of PhIO added to each reaction. Control reactions, in the absence of iron(III) porphyrins, were also carried out using the methodology described above. The solid **FeP3S** was recovered after the first use, washed with methanol, acetonitrile and dichloromethane and, after drying, the solid was reused in other catalytic cycles using (*Z*)-cyclooctene as substrate. The resulting washing solutions of the recovered catalyst were analyzed by UV-Vis to evaluate the possible solubilization of the iron(III) porphyrin unit.

Physical measurements

Electronic spectra (UV-Vis), both of solutions and of the solid samples, were obtained on a Cary-Varian UV-Vis spectrophotometer in the 350–800 nm range. Attenuated Total Reflectance Transmission Fourier Transform Infrared (ATR-FTIR) spectra were registered on a FT Mattson 7000 galaxy series spectrophotometer in the 400–4000 cm^{-1} range, and the spectra were collected with a resolution of 4 cm^{-1} and accumulation of 32 scans. Electron Paramagnetic Resonance (EPR) measurements of the powder materials (solid sample) were accomplished on an EPR BRUKER EMX microX spectrometer (frequency X, band 9.5 GHz) at 77 K (using liquid N_2). The organic products from the catalytic oxidation reactions and the remaining substrates were identified and quantified using an Agilent 6850 (FID detector) gas chromatograph equipped with a DB-WAX capillary column (J&W Scientific, 30 μm × 0.25 mm i.d., 0.25 μm film thickness) using nitrogen as the carrier gas. The oven temperature program used to determine the oxidation products from (Z)-cyclooctene and cyclohexane started at 100 °C; the temperature was then increased to 150 °C at 10 °C min^{-1}, followed by further temperature rise to 200 °C at 50 °C min^{-1} (maintained for 1 min). For heptane products detection, the temperature program started at 70 °C, followed by a temperature raise to 100 °C at 5 °C min^{-1} (maintained for 1 min), and then the temperature was increased to 200 °C at 20 °C min^{-1} (maintained for 1 min). The injector and detector temperatures were fixed at 200 °C and 250 °C, respectively, for all the analyses). The oxidation products were identified using standards. Quantitative analysis was carried out by standard internal methodology.

3. Conclusions

Porphyrin **H_2P2** containing the protected sugar dendrimers R^2 (Scheme 1) allowed the synthesis of a new iron(III) porphyrin **FeP2** after metalation with an excess of iron(II) chloride. The presence of the isopropylidene protective groups (R^2) avoided the formation of any aggregated network. The afforded **FeP2** remained soluble in the different solvents tested in this work, similarly to **FeP1**. On the other hand, the presence of unprotected glycodendrimers (R^3) substituents in the structure of porphyrin **H_2P3** allowed the preparation of a solid and insoluble new material when the free-base porphyrin was used to prepare the iron(III) porphyrin with an excess of iron(II) chloride. The characterization of the resulting insoluble solid **FeP3S** suggested that probably the coordination of iron(III) ions to the dendritic units R^3 took place, thus resulting in an insoluble solid hybrid material. The characteristics of **FeP3S** suggest that this is a structured solid network similar to that

observed previously by us when copper(II) ions were used to metalate the free-base **H_2P3**.

The introduction of the glycodendrimer substituents (R^2 and R^3) at the *p*-positions of the *meso*-aryl groups of the porphyrin macrocycle could fine-tune the catalytic efficiency, selectivity, and regioselectivity of the resulting compounds/materials. In fact, we showed that it is possible to modulate the selectivity and chemical efficiency of catalytic systems by choosing the appropriate substituent. The presence of bulky groups and the putative presence of small channels and pores in the solid **FeP3S** has restricted the access to catalysis of larger substrates. **FeP2** and **FeP3S** display a very promising catalytic activity for heptane oxidation.

For **FeP3S** we were able to demonstrate that it is possible to modulate catalytic activity and selectivity by choice of the solvent and the time of reaction for heptane oxidation. Furthermore, the reuse of **FeP3S** in the oxidation of (*Z*)-cyclooctene did not lead to inactivation of the catalyst during the reaction or washing processes. The successful recovery and reuse of this **FeP3S** catalyst, along with the results obtained for the oxidation of an inert substrate such as heptane, directs us for future investigations with other inert substrates.

Acknowledgments

The authors are grateful to Coordenação de Aperfeiçoamento de Pessoal de Nível Superior (CAPES – Finance code 001) and CAPES/PrInt (Process 88881.311981/2018-01), Conselho Nacional de Desenvolvimento Científico e Tecnológico – CNPq (S. Nakagaki Process 405217/2018-8), Fundação Araucária, Centro de Microscopia da UFPR, Universidade Federal do Paraná (FUNPAR), and Universidade Federal do Paraná – UFPR for the financial support. Additional acknowledgement is due to the University of Aveiro and FCT/MCTES (Fundacão para a Ciência e Tecnologia and Ministério da Ciência, Tecnologia e Ensino Superior) and European Union (COMPETE and FEDER programs) for the financial support to UIDB/50006/2020 (LAQV-REQUIMTE) and CQE (UIDB/00100/2020) research units, through national funds and, where applicable, co-financed by FEDER, within the PT2020 Partnership Agreement. Kelly A. D. F. Castro also thanks CNPq for her post-doctoral scholarship (Process 151512/2013-2). Kátia C. M. Westrup also thanks Fundação Araucária and CAPES for her post-doctoral scholarship (Agreement 396/2014 – Project 41060). The authors also acknowledge FCT for the doctoral research fellowship SFRH/BD/85941/2012 (to PMRP).

Conflict of Interest

The authors declare no conflict of interest.

Keywords: Catalysis · Oxidation · Porphyrin · Selectivity · Sugar dendrimers

[1] a) R. A. Smith, *J. Chem. Educ.* **1998**, *75*, 1–420; b) K. Kadish, K. M. Smith, R. Guilard in, *The Porphyrin Handbook*, Academic Press, **1999**, vol. 4.

[2] a) P. M. R. Pereira, N. Berisha, N. V. S. D. K. Bhupathiraju, R. Fernandes, J. P. C. Tomé, C. M. Drain, *PLoS One* **2017**, *12*, 1–21; b) F. Figueira, P. M. R. Pereira, S. Silva, J. A. S. Cavaleiro, J. P. C. Tomé, *Curr. Org. Synth.* **2014**, *11*, 110–126; c) H. Abrahamse, M. R. Hamblin, *Biochem. J.* **2016**, *473*, 347–364; d) R. Bonnett, *Rev. Contemp. Pharmacother.* **1999**, *10*, 1–17; e) F. Bryden, R. W. Boyle, *Adv. Inorg. Chem.* **2016**, *68*, 141–221; f) Y. Ni, *Curr. Med. Imaging Rev.* **2008**, *4*, 96–112; g) B. M. Amos-Tautua, S. P. Songca, O. S. Oluwafemi, *Molecules* **2019**, *24*, 2456; h) M. Q. Mesquita, C. J. Dias, S. Gamelas, M. Fardilha, M. G. P. M. S. Neves, M. A. F. Faustino, *An. Acad. Bras. Cienc.* **2018**, *90*, 1101–1130; i) N. Tsolekile, S. Nahle, N. Zikalala, S. Parani, E. H. M. Sakho, O. Joubert, M. C. Matoetoe, S. P. Songca, O. S. Oluwafemi, *Sci. Rep.* **2020**, *10*, 4936; j) K. A. D. F. Castro, N. M. M. Moura, A. Fernandes, M. A. F. Faustino, M. M. Q. Simões, J. A. S. Cavaleiro, S. Nakagaki, A. Almeida, A. Cunha, A. J. D. Silvestre, C. S. R. Freire, R. J. B. Pinto, M. G. P. M. S. Neves, *Dyes Pigm.* **2017**, *137*, 265–276; k) C. Simões, M. C. Gomes, M. G. P. M. S. Neves, A. Cunha, J. P. C. Tomé, A. C. Tomé, J. A. S. Cavaleiro, A. Almeida, M. A. F. Faustino, *Catal. Today* **2016**, *266*, 197–204; l) P. M. R. Pereira, J. J. Carvalho, S. Silva, J. A. S. Cavaleiro, R. J. Schneider, R. Fernandes, J. P. C. Tomé, *Org. Biomol. Chem.* **2014**, *12*, 1804–1811; m) N. V. S. D. K. Bhupathiraju, W. Rizvi, J. D. Batteas, C. M. Drain, *Org. Biomol. Chem.* **2016**, *14*, 389–408; n) J. Yoho, K. Wogensthal, T. L. Bennett, J. Palmer, K. K. Comfort, M. Kango-Singh, S. Swavey, C. H. Stuart, W. H. Gmeiner, *Eur. J. Inorg. Chem.* **2017**, *2017*, 153–159.

[3] a) R. M. Ion, V. A. Faraon, R. M. Senin, R. C. Fierascu, *React. Kinet. Mech. Catal.* **2016**, *118*, 337–348; b) C. F. Pereira, M. M. Q. Simões, J. P. C. Tomé, F. A. A. Paz, *Molecules* **2016**, *21*, 1348; c) K. A. D. F. Castro, M. M. Q. Simões, M. G. P. M. S. Neves, J. A. S. Cavaleiro, F. Wypych, S. Nakagaki, *Catal. Sci. Technol.* **2014**, *4*, 129–141; d) S. Nakagaki, K. A. D. F. Castro, M. G. P. M. S. Neves, M. A. F. Faustino, Y. Iamamoto, *J. Braz. Chem. Soc.* **2019**, *30*, 2501–2535; e) K. C. M. Westrup, R. M. da Silva, K. M. Mantovani, L. Bach, J. F. Stival, P. G. P. Zamora, F. Wypych, G. S. Machado, S. Nakagaki, *Appl. Catal. A* **2020**, *602*, 117708; f) K. A. D. F. Castro, M. M. Q. Simões, M. G. P. M. S. Neves, J. A. S. Cavaleiro, R. R. Ribeiro, F. Wypych, S. Nakagaki, *Appl. Catal. A* **2015**, *503*, 9–19; g) K. A. D. F. Castro, S. Silva, P. M. Pereira, M. M. Q. Simões, M. G. P. M. S. Neves, J. A. S. Cavaleiro, F. Wypych, J. P. Tomé, S. Nakagaki, *Inorg. Chem.* **2015**, *54*, 4382–4393; h) F. B. Zanardi, I. A. Barbosa, P. C. de Sousa, L. D. Zanatta, D. L. da Silva, O. A. Serra, Y. Iamamoto, *Microporous Mesoporous Mater.* **2016**, *219*, 161–171; i) J. R. L. Smith, Y. Iamamoto, F. S. Vinhado, *J. Mol. Catal. A* **2006**, *252*, 23–30; j) J. C. Barona-Castano, C. C. Carmona-Vargas, T. J. Brocksom, K. T. de Oliveira, *Molecules* **2016**, *21*, 310; k) D. Mansuy, *C. R. Chim.* **2007**, *10*, 392–413; l) J. T. Groves, *J. Inorg. Biochem.* **2006**, *100*, 434–447; m) J. Bernadou, B. Meunier, *Adv. Synth. Catal.* **2004**, *346*, 171–184; n) D. R. Leanord, J. R. L. Smith, *J. Chem. Soc. Perkin Trans. 2* **1990**, 1917–1923; o) K. Anjali, M. S. Aswini, P. Aswin, V. Ganesh, A. Sakthivel, *Eur. J. Inorg. Chem.* **2019**, *2019*, 4087–4094; p) A. Molinari, R. Amadelli, V. Carassiti, A. Maldotti, *Eur. J. Inorg. Chem.* **2000**, *2000*, 91–96.

[4] a) P. T. Anastas, M. M. Kirchhoff, T. C. Williamson, *Appl. Catal. A* **2001**, *221*, 3–13; b) B. A. de Marco, B. S. Rechelo, E. G. Totoli, A. C. Kogawa, H. R. N. Salgado, *Saudi Pharm. J.* **2019**, *27*, 1–8; c) P. T. Anastas, J. C. Warner, *Green chemistry: theory and practice*, Oxford University Press, Oxford [England]; New York, **1998**, p. 1–152.

[5] R. A. Sheldon, *J. Chem. Technol. Biotechnol.* **1997**, *68*, 381–388.

[6] J. C. Vedrine, *Catalysts* **2016**, *6*, 22.

[7] a) S. Nakagaki, G. K. B. Ferreira, G. M. Ucoski, K. A. D. D. Castro, *Molecules* **2013**, *18*, 7279–7308; b) G. Wegener, M. Brandt, L. Duda, J. Hofmann, B. Klesczewski, D. Koch, R.-J. Kumpf, H. Orzesek, H.-G. Pirkl, C. Six, C. Steinlein, M. Weisbeck, *Appl. Catal. A* **2001**, *221*, 303–335.

[8] G. Bellussi, C. Perego, *CATTECH* **2000**, *4*, 4–16.

[9] J. M. Thomas, R. Raja, G. Sankar, R. G. Bell, *Acc. Chem. Res.* **2001**, *34*, 191–200.

[10] a) K. A. D. F. Castro, F. Figueira, R. F. Mendes, J. A. S. Cavaleiro, M. G. P. M. S. Neves, M. M. Q. Simões, F. A. A. Paz, J. P. C. Tomé, S. Nakagaki, *ChemCatChem* **2017**, *9*, 2939–2945; b) K. S. Suslick, B. R. Cook, *J. Chem. Soc. Chem. Commun.* **1987**, 200–202.

[11] a) M. M. Q. Simões, C. M. B. Neves, S. M. G. Pires, M. G. P. M. S. Neves, J. A. S. Cavaleiro, *Pure Appl. Chem.* **2013**, *85*, 1671–1681; b) M. Halma, K. A. D. F. Castro, C. Taviot-Gueho, V. Prévot, C. Forano, F. Wypych, S. Nakagaki, *J. Catal.* **2008**, *257*, 233–243; c) G. M. Ucoski, V. H. A. Pinto, G. DeFreitas-Silva, J. S. Rebouças, R. M. da Silva, I. Mazzaro, F. S. Nunes, S. Nakagaki, *Microporous Mesoporous Mater.* **2018**, *265*, 84–97; d) K. A. D. F. Castro, F. H. C. de Lima, M. M. Q. Simões, M. G. P. M. S. Neves, F. A. A.

Paz, R. F. Mendes, S. Nakagaki, J. A. S. Cavaleiro, *Inorg. Chim. Acta* **2017**, *455*, 575–583; e) A. R. Antonangelo, C. G. Bezzu, N. B. McKeown, S. Nakagaki, *J. Catal.* **2019**, *369*, 133–142; f) O. Fazio, M. Gnida, W. Meyer-Klaucke, W. Frank, W. Kläui, *Eur. J. Inorg. Chem.* **2002**, *2002*, 2891–2896.

[12] a) Q. Liu, C. C. Guo, *Sci. China Chem.* **2012**, *55*, 2036–2053; b) C. C. Guo, X. Q. Liu, Q. Liu, Y. Liu, M. F. Chu, W. Y. Lin, *J. Porphyrins Phthalocyanines* **2009**, *13*, 1250–1254.

[13] a) B. Meunier, *Chem. Rev.* **1992**, *92*, 1411–1456; b) B. Meunier, S. P. de Visser, S. Shaik, *Chem. Rev.* **2004**, *104*, 3947–3980; c) D. Dolphin, T. G. Traylor, L. Y. Xie, *Acc. Chem. Res.* **1997**, *30*, 251–259; d) A. R. Antonangelo, K. C. M. Westrup, L. A. Burt, C. G. Bezzu, T. Malewschik, G. S. Machado, F. S. Nunes, N. B. McKeown, S. Nakagaki, *RSC Adv.* **2017**, *7*, 50610–50618.

[14] a) M. J. Nappa, C. A. Tolman, *Inorg. Chem.* **1985**, *24*, 4711–4719; b) K. S. Suslick, P. Bhyrappa, J. H. Chou, M. E. Kosal, S. Nakagaki, D. W. Smithenry, S. R. Wilson, *Acc. Chem. Res.* **2005**, *38*, 283–291.

[15] S. Silva, P. M. R. Pereira, P. Silva, F. A. A. Paz, M. A. F. Faustino, J. A. S. Cavaleiro, J. P. C. Tomé, *Chem. Commun.* **2012**, *48*, 3608–3610.

[16] L. J. Boucher, *J. Am. Chem. Soc.* **1970**, *92*, 2725–2730.

[17] a) J. L. Nian, L. Min, H. A. Kong, *Inorg. Chim. Acta* **1990**, *178*, 59–65; b) M. Gouterman, *J. Mol. Spectrosc.* **1961**, *6*, 138–163.

[18] J. Sebestik, P. Niederhafner, J. Jezek, *Amino Acids* **2011**, *40*, 301–370.

[19] L. Nagy, K. Burger, J. Kürti, M. A. Mostafa, L. Korecz, I. Kiricsi, *Inorg. Chim. Acta* **1986**, *124*, 55–59.

[20] a) R. P. Bandwar, M. S. Srinivasa Raghavan, C. P. Rao, *BioMetals* **1995**, *8*, 19–24; b) K. Geetha, M. S. S. Raghavan, S. K. Kulshreshtha, R. Sasikala, C. P. Rao, *Carbohydr. Res.* **1995**, *271*, 163–175.

[21] S. Yano, *Coord. Chem. Rev.* **1988**, *92*, 113–156.

[22] K. A. D. F. Castro, F. Figueira, R. F. Mendes, F. A. Almeida Paz, M. G. P. M. S. Neves, J. A. S. Cavaleiro, S. Nakagaki, J. P. C. Tomé, M. M. Q. Simões, *Polyhedron* **2019**, *158*, 478–484.

[23] R. Zhang, Y. Liu, Y. An, Z. Wang, P. Wang, Z. Zheng, X. Qin, X. Zhang, Y. Dai, B. Huang, *Colloids Surf. A* **2019**, *560*, 315–322.

[24] a) N. A. Stephenson, A. T. Bell, *J. Am. Chem. Soc.* **2005**, *127*, 8635–8643; b) N. A. Stephenson, A. T. Bell, *Inorg. Chem.* **2006**, *45*, 2758–2766; c) M. Nakamura, *Coord. Chem. Rev.* **2006**, *250*, 2271–2294.

[25] a) J. Kürti, M. A. Mostafa, L. Korecz, L. Nagy, K. Burger, *J. Radioanal. Nucl. Chem.* **1987**, *118*, 437–448; b) A. L. R. Mercê, E. Fernandes, A. S. Mangrich, M. R. Sierakowski, B. Szpoganicz, *J. Braz. Chem. Soc.* **2001**, *12*, 791–798.

[26] a) J. T. Weisser, M. J. Nilges, M. J. Sever, J. J. Wilker, *Inorg. Chem.* **2006**, *45*, 7736–7747; b) E. A. Zhilinskaya, G. Delahay, M. Mauvezin, B. Coq, A. Aboukaïs, *Langmuir* **2003**, *19*, 3596–3602; c) R. Naik, S. C. Prashantha, H. Nagabhushana, K. M. Girish, *J. Lumin.* **2018**, *197*, 233–241.

[27] C. P. Rao, K. Geetha, M. S. S. Raghavan, *BioMetals* **1994**, *7*, 25–29.

[28] a) Y. Iamamoto, M. D. Assis, K. J. Ciuffi, H. C. Sacco, L. Iwamoto, A. J. B. Melo, O. R. Nascimento, C. M. Prado, *J. Mol. Catal. A* **1996**, *109*, 189–200; b) S. L. H. Rebelo, A. M. N. Silva, C. J. Medforth, C. Freire, *Molecules* **2016**, *21*, 481.

[29] K. B. Vu, T. K. Phung, *J. Ind. Eng. Chem.* **2016**, *40*, 40–46.

[30] a) W. Nam, H. J. Lee, S.-Y. Oh, C. Kim, H. G. Jang, *J. Inorg. Biochem.* **2000**, *80*, 219–225; b) P. Bhyrappa, J. K. Young, J. S. Moore, K. S. Suslick, *J. Am. Chem. Soc.* **1996**, *118*, 5708–5711.

[31] F. S. Vinhado, M. E. F. Gandini, Y. Iamamoto, A. M. G. Silva, M. M. Q. Simões, M. G. P. M. S. Neves, A. C. Tomé, S. L. H. Rebelo, A. M. V. M. Pereira, J. A. S. Cavaleiro, *J. Mol. Catal. A* **2005**, *239*, 138–143.

[32] a) A. A. Alshaheri, M. I. M. Tahir, M. B. A. Rahman, T. B. S. A. Ravoof, T. A. Saleh, *Chem. Eng. J.* **2017**, *327*, 423–430; b) S. Khare, P. Shrivastava, R. Chokhare, J. S. Kirar, S. Parashar, *J. Porous Mater.* **2017**, *24*, 855–866.

[33] a) H. Arakawa, M. Aresta, J. N. Armor, M. A. Barteau, E. J. Beckman, A. T. Bell, J. E. Bercaw, C. Creutz, E. Dinjus, D. A. Dixon, K. Domen, D. L. DuBois, J. Eckert, E. Fujita, D. H. Gibson, W. A. Goddard, D. W. Goodman, J. Keller, G. J. Kubas, H. H. Kung, J. E. Lyons, L. E. Manzer, T. J. Marks, K. Morokuma, K. M. Nicholas, R. Periana, L. Que, J. Rostrup-Nielson, W. M. Sachtler, L. D. Schmidt, A. Sen, G. A. Somorjai, P. C. Stair, B. R. Stults, W. Tumas, *Chem. Rev.* **2001**, *101*, 953–996; b) R. Raja, G. Sankar, J. M. Thomas, *Angew. Chem. Int. Ed. Engl.* **2000**, *39*, 2313–2316.

[34] X. Tang, X. Jia, Z. Huang, *Chem. Sci.* **2018**, *9*, 288–299.

[35] a) G. K. B. Ferreira, K. A. D. d F Castro, G. S. Machado, R. R. Ribeiro, K. J. Ciuffi, G. P. Ricci, J. A. Marques, S. Nakagaki, *J. Mol. Catal. A* **2013**, *378*, 263–272; b) M. Thomas, J. C. Hernandez-Garrido, R. Raja, R. G. Bell, *Phys. Chem. Chem. Phys.* **2009**, *11*, 2799–2825.

[36] S. Van de Vyver, Y. Román-Leshkov, *Catal. Sci. Technol.* **2013**, *3*, 1465–1479.

[37] a) P. Battioni, E. Cardin, M. Louloudi, B. Schöllhorn, G. A. Spyroulias, D. Mansuy, T. G. Traylor, *Chem. Commun.* **1996**, 2037–2038; b) F. Bartoli, O. Brigaud, P. Battioni, D. Mansuy, *J. Chem. Soc. Chem. Commun.* **1991**, 440–442; c) M. Bordeaux, A. Galarneau, J. Drone, *Angew. Chem. Int. Ed.* **2012**, *51*, 2–14; *Angew. Chem.* **2012**, *124*, 2–2.

[38] M. A. Martinez-Lorente, P. Battioni, W. Kleemiss, J. F. Bartoli, D. Mansuy, *J. Mol. Catal. A* **1996**, *113*, 343–353.

[39] B. R. Cook, T. J. Reinert, K. S. Suslick, *J. Am. Chem. Soc.* **1986**, *108*, 7281–7286.

[40] H. Y. Thu, G. S. Tong, J. S. Huang, S. L. Chan, Q. H. Deng, C. M. Che, *Angew. Chem. Int. Ed. Engl.* **2008**, *47*, 9747–9751.

[41] V. H. A. Pinto, N. Falcao, B. Mariz-Silva, M. G. Fonseca, J. S. Reboucas, *Dalton Trans.* **2020**, *49*, 16404–16418.

[42] L. Barloy, P. Battioni, D. Mansuy, *J. Chem. Soc. Chem. Commun.* **1990**, 1365–1367.

[43] P. Battioni, J.-P. Lallier, L. Barloy, D. Mansuy, *J. Chem. Soc. Chem. Commun.* **1989**, 1149–1151.

[44] J. F. Bartoli, O. Brigaud, P. Battioni, D. Mansuy, *J. Chem. Soc. Chem. Commun.* **1991**, 440–442.

[45] H. Saltzman, J. G. Sharefkin, *Org. Synth.* **1963**, *43*, 60–60.

[46] H. J. Lucas, E. R. Kenedy, M. W. Formo, *Org. Synth.* **1942**, *22*, 70.

[47] H. Kobayashi, T. Higuchi, Y. Kaizu, H. Osada, M. Aoki, *B. Chem. Soc. Jpn.* **1975**, *48*, 3137–3141.

[48] K. A. D. F. Castro, S. M. G. Pires, M. A. Ribeiro, M. M. Q. Simões, M. G. P. M. S. Neves, W. H. Schreiner, F. Wypych, J. A. S. Cavaleiro, S. Nakagaki, *J. Colloid Interface Sci.* **2015**, *450*, 339–352.

Manuscript received: April 29, 2021
Revised manuscript received: June 21, 2021